ACS APPLIED MATERIALS & INTERFACES

Research Article

www.acsami.org

Molecular Flux Dependence of Chemical Patterning by Microcontact Printing

Jeffrey J. Schwartz,[†,‡] J. Nathan Hohman,[†,§,⊥] Elizabeth I. Morin,[§] and Paul S. Weiss*[,†,§,⊥,#]

[†]California NanoSystems Institute and [‡]Department of Physics and Astronomy, University of California, Los Angeles, Los Angeles, California 90095, United States

[§]Department of Chemistry, The Pennsylvania State University, University Park, Pennsylvania 16802, United States

[⊥]Department of Chemistry and Biochemistry and [#]Department of Materials Science and Engineering, University of California, Los Angeles, Los Angeles, California 90095, United States

ABSTRACT: We address the importance of the dynamic molecular ink concentration at a polymer stamp/substrate interface during microcontact displacement or insertion printing. We demonstrate that by controlling molecular flux, we can influence both the molecular-scale order and the rate of molecular exchange of self-assembled monolayers (SAMs) on gold surfaces. Surface depletion of molecular ink at a polymer stamp/substrate interface is driven predominantly by diffusion into the stamp interior; depletion occurs briefly at the substrate by SAM formation, but diffusion of molecules into the bulk of the stamp dominates over practical experimental time scales. As contact time is increased, the interface concentration varies significantly due to diffusion, affecting the quality and coverage of printed films. Controlling interfacial concentration improves printed film reproducibility and the fractional coverage of multicomponent films can be controlled to within a few percent. We first briefly review the important aspects of molecular ink diffusion at a stamp interface and how it relates to experimental duration. We then describe two examples that illustrate control over ink transfer during experiments: the role of contact time on monolayer reproducibility and molecular order, and the fine control of fractional monolayer coverage for the displacement printing of 1-adamantanethiolate SAMs by 1-dodecanethiol.

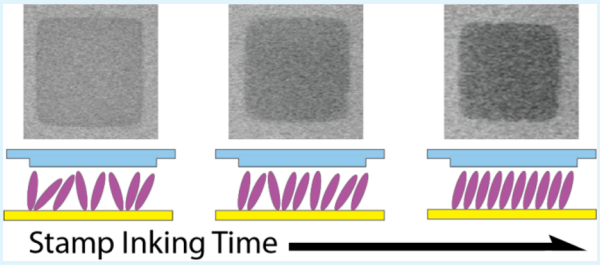

KEYWORDS: *microcontact printing, microdisplacement printing, nanoscale patterning, self-assembled monolayers, scanning electron microscopy, infrared reflection absorption spectroscopy*

INTRODUCTION

Microcontact printing (μCP) enables parallel soft-lithographic patterning of materials ranging from small-molecule inks to nanoparticles.[1−15] In its simplest form, an elastomeric stamp with a relief pattern is dosed with ink molecules (inked) and then is placed in conformal contact with a reactive surface.[16−25] Molecules, henceforth referred to simply as "ink," transfer from stamp to substrate and, in the cases of thiol inks on many metals, form self-assembled monolayers (SAMs), imbuing the contact sites with the chemical properties of the molecular assembly. The key advantages of μCP are its flexibility and intrinsic simplicity; the inking method, substrate, and stamp can be tailored to produce the desired results. For example, ink pads can be used to limit swelling of the elastomeric stamp by solvent absorption,[26] the stamp surface can be hydrophilized by UV/ozone or oxygen plasma treatment to modulate ink transfer between stamp and substrate,[27−30] or the stamp may be functionalized to catalyze reactions on the substrate.[31−35] Generally, μCP procedures for printing *n*-alkanethiol inks on noble metals call for short contact times; a bare gold surface is sufficiently reactive to thiols that nearly full coverage films are produced after contact times on the millisecond scale.[36,37]

We have previously reported methods for controlling ink transfer by modulating the reactivity of substrates through the use of preformed SAMs.[38−41] Microdisplacement (μDP) printing utilizes the exchange of *n*-alkanethiols with a preformed **1AD** SAM.[38,42−48] Time scales for μDP experiments are typically an order of magnitude longer than those for μCP experiments, ranging from 15 min to 24 h, depending on the ink employed and the desired coverage. Controlling the molecular flux (defined as the quantity of molecules delivered to the interface by diffusion) at the stamp/substrate interface becomes imperative when printing time scales are comparable to, or exceed, inking times.

EXPERIMENTAL SECTION

Materials and Methods. Undoped, single-side polished Si(100) wafers (<40 Ω cm resistivity, 350−400 μm thickness) were used as received from Silicon Quest International. Thiols (1-dodecanethiol, **C12**; 1-octadecanethiol, **C18**; and 1-adamantanethiol, **1AD**), hexanes, and ethanol were all used as received from Sigma Aldrich. Deionized

Received: August 6, 2013
Accepted: September 26, 2013
Published: September 26, 2013

water (18.2 MΩ cm) was dispensed by a Milli-Q system purchased from Millipore (Billerica, MA, USA). Sylgard 184 Base and PDMS Sylgard 184 Cure were obtained from Dow Corning (Midland, MI, USA). Heptadecafluoro-1,1,2,2-tetra-hydrodecyl trichlorosilane was used as received from Gelest (Morrisville, PA, USA).

Preparation of Polymer Stamps. Patterned polydimethylsiloxane (PDMS) stamps were prepared from photolithographically defined features etched into a silicon wafer. An unpatterned wafer was used to prepare flat stamps. Before the first use of the silicon masters, they were treated with (heptadecafluoro-1,1,2,2-tetra-hydrodecyl) trichlorosilane to prevent PDMS adhesion to the silicon. A small quantity (~0.1 mL) of the chemical was deposited on a glass coverslip in a vacuum desiccator, alongside the silicon masters, and a vacuum (1×10^{-2} Torr) was drawn until the chemical evaporated. Afterward, the wafers were rinsed serially with acetone and ethanol, and then dried with nitrogen gas.

The PDMS Sylgard 184 Base and PDMS Sylgard 184 Cure were combined in a 10:1 ratio (by weight) and stirred vigorously. The mixed prepolymer, in a disposable plastic container with tall sides, was placed in a vacuum desiccator and deaerated under vacuum (1×10^{-3} Torr) until no bubbles were visible (the mixed polymer expands substantially under reduced pressure as trapped gas bubbles expand in volume). The deaerated polymer was poured over the silicon masters in a foil-lined Petri dish. The dish is deaerated to remove any residual or introduced bubbles. Afterward, the PDMS was cured at 60 °C for 24 h. Stamps were then peeled from the silicon master and cut to the desired size with a razor blade.

Low molecular weight PDMS is removed by swelling cured stamps in hexanes for 6 h, replacing the hexanes every 2 h. Swelled stamps are heated at 40 °C for at least 24 h. As the hexane evaporates, the stamps shrink to their original size. Stamps can crack if they are laid flat on a surface, or if the temperature is too high, during baking. The stamp surface can be cleaned by sonication for 30 min in a 1:1 water/ethanol bath. Stamps are then dried with a stream of nitrogen and stored face up in a plastic Petri dish until needed.

Stamp Inking. The traditional wet-inking method, common among many variations of μCP experiments, involves pipetting an ethanolic solution of an alkanethiol ink onto the stamp surface, where it sits for 10 to 60 s. After the desired inking time has elapsed (usually 60 s) the stamp is blown dry with a stream of nitrogen.

For saturation inking, a stamp is immersed in an ethanolic solution of the appropriate concentration for an order of magnitude longer than the printing time scale. Upon removal from solution, the stamp is briefly rinsed with neat ethanol and dried with nitrogen gas. Rinsing the stamp minimizes surface crystallization for high-molecular-weight inks. Thinner stamps (<5 mm) reach saturation more quickly than thicker stamps.

Printing. The PDMS stamps will generally adhere to flat surfaces, so it is convenient to center the stamp on a polished metal disk (here 60 g) to act as a weight, bringing the stamp/weight combination in contact with a surface in a single motion. Twisting or other motions result in smudged or doubled patterns. After the desired contact time, the weight and sample are removed together. The sample is rinsed with neat ethanol and dried with a stream of nitrogen.

For IR analysis, the substrate must be uniformly printed. To prepare these samples, an inked, featureless stamp is brought into contact with a substrate to form complete monolayers. It is most convenient to print with a stamp that is slightly larger than the sample.

Grazing Incidence IR Spectroscopy. Infrared spectra were collected using a Nicolet 6700 FTIR spectrometer (Thermo Electron Corp., Waltham, MA), equipped with a liquid-nitrogen-cooled mercury−cadmium-telluride detector and a Seagull variable-angle reflection accessory (Harrick Scientific, Inc., Ossining, NY). A FTIR Purge Gas Generator (Parker-Balston, Cleveland, OH) removed water and CO_2 from the gas stream used to purge the spectrometer and its accessory. The data were collected at grazing incidence reflection (82° relative to the surface normal) with *p*-polarized light and a mirror speed of 1.27 cm s^{-1}, with a resolution of 2 cm^{-1}. All spectra were averaged over 1024 scans. Scans were normalized with spectra of perdeuterated *n*-dodecanethiolate monolayers on Au{111}.

Scanning Electron Microscopy. Scanning electron micrographs of patterned **1AD/C12** SAMs were collected using a Leo 1530 field-emission scanning electron microscope (SEM) at an accelerating voltage of 5 kV. We have previously shown that the SEM is sensitive to exposed chemical functionality and chemical patterns.[47]

RESULTS AND DISCUSSION

Infrared Spectroscopy of Printed Films. Infrared reflectance adsorption spectroscopy (IRRAS) is an ensemble technique used to determine SAM structural and compositional details. Self-assembled monolayer order improves with increasing deposition time. A SAM formed only briefly is a kinetic product with a high defect density.[49,50] Exchange between molecules in solution and those on the surface tends to increase average domain size, resulting in SAMs with higher degrees of order.[42,51] Figure 1 shows four offset IR spectra for SAMs printed with varying contact times by a featureless slab of PDMS ("flat stamp"), saturation-inked for 24 h with 25 mM **C12**.

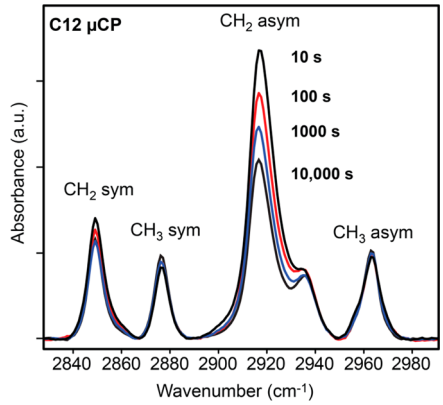

Figure 1. Infrared reflection absorbance spectra of the methyl (CH_3) and methylene (CH_2) stretches present in 1-dodecanethiol self-assembled monolayers (SAMs) on gold, prepared by microcontact printing with contact times varying by orders of magnitude. All four spectra are characteristic of full-coverage, crystalline SAMs, but the decrease in CH_2 asymmetric stretch intensity with printing time correlates to an improvement in overall order and uniformity of the film. The stamps are featureless PDMS slabs, saturation-inked in a 25 mM ethanolic solution of 1-dodecanethiol for 24 h prior to printing.

Infrared spectra of *n*-alkanethiolate SAMs show five characteristic peaks associated with hydrocarbon chains between 2800 and 3000 cm^{-1}, of which two are relevant diagnostically. The methylene (CH_2) asymmetric stretch is the dominant spectral feature and is found between 2918 and 2920 cm^{-1}. This stretch is highly sensitive to monolayer crystallinity. The peak shifts toward 2918 cm^{-1} for crystalline, solidlike films.[52] Disordered areas are more liquidlike, and the peak shifts to higher wavenumbers (higher energies).

Application of surface selection rules helps elucidate the structure and orientation of molecules at interfaces. Infrared radiation excites those vibrational modes that result in changes in the transition dipole moment; on conductive surfaces, absorption is maximized if the dipole is oriented normal to the surface and is attenuated if parallel to the surface.[53] Molecules in well-ordered domains are tilted uniformly from the surface normal by 30°, a configuration that tends to decrease infrared adsorption intensity of the CH_2 asymmetric stretch. Disordered molecules have more orientational degrees of freedom,

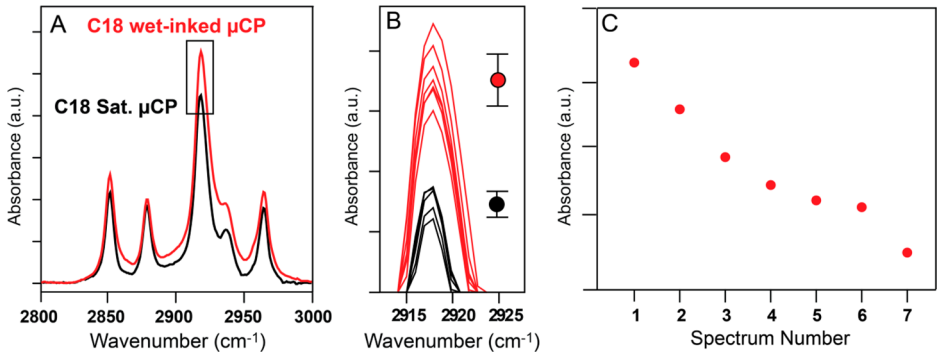

Figure 2. Increasing inking time results in a corresponding improvement in printed monolayer order and minimizes variability between experiments. (A) Representative infrared spectra for printed 1-octadecanethiol (**C18**) self-assembled monolayers (SAMs). Stamps were either sequentially wet-inked for 1 min (red trace) or saturation inked for 24 h (black trace). The methylene asymmetric stretch (2919 cm^{-1}) intensity correlates inversely to film quality; SAMs printed by saturation-inking show consistently higher conformational order than wet-inked films. (B) Expanded view of the boxed area in A, which shows an overlay of all spectra in the data set. The mean and standard deviation of each series are denoted by the black and red circles, which correspond to the saturation-inked and wet-inked series, respectively, and illustrate the superior control provided by the saturation-inking method. (C) Repeated wet-inking between prints increases the absolute ink loading of a stamp. Plotting the 2919 cm^{-1} peak height of the wet-inked series against the preparation sequence reveals consistent improvement in film quality. Each time the stamp is inked, the absolute ink loading increases, which in turn improves the conformational order of the printed SAMs.

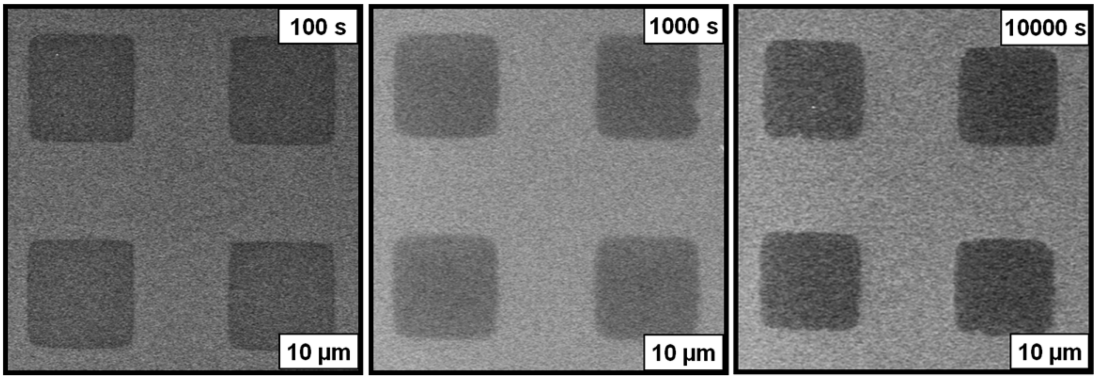

Figure 3. Scanning electron micrographs of chemical patterns produced by microdisplacement printing on a preformed 1-adamantanethiol self-assembled monolayer by contact with a stamp saturation-inked with 25 mM 1-dodecanethiol. Absolute coverage increases with contact time and the contrast between the pattern and background shifts (but cannot be estimated by scanning electron microscopy without an internal reference). Based on the observed patterns, we assign the higher intensity regions (shown as brighter) evident in each of the above images to be the 1-adamantanethiol preformed monolayer, while areas where 1-dodecanethiol (molecular ink deposited by the stamp) displaced 1-adamantanethiol molecules in the monolayer appear as lower intensity regions.

resulting in an average increase in the absorption intensity of the methylene modes. This effect can be seen in Figure 1; as contact time increases logarithmically, CH_2 asymmetric intensity decreases linearly.[54]

The methyl (CH_3) symmetric stretch is an excellent indicator of absolute *n*-alkanethiolate coverage; IR adsorption is relatively insensitive to the orientation of the methyl group, compared to CH_2 orientation, once assembled into a SAM.[42,52] Printed SAMs can be expected to have >90% coverage within the first second of contact. The methyl symmetric stretch intensity increases by <8% during the 9000 s period that followed the first 1000 s of contact time. Other spectral features are the CH_2 symmetric, the CH_3 asymmetric, and the minor CH_3 Fermi resonance at 2850, 2990, and 2935 cm^{-1}, respectively.[52]

Monitoring and Controlling the Degree of Order of Printed Monolayers. Two series of samples were prepared and their IR spectra compared to test the reproducibility of conformational order in printed films. The first series was prepared using a stamp that was wet-inked for 1 min with 25 mM ethanolic **C18** solution. The second series was prepared from a stamp that was saturation-inked by immersion in a 25 mM ethanolic **C18** solution for 24 h. Both sets were prepared using virgin, featureless PDMS slabs that uniformly cover a sample surface, with a printing contact time of 15 min for SAM formation. The stamps were reinked between each printing. The results of these experiments are shown in Figure 2.

The uniformity of printed SAMs is dependent on both the inking and the printing times. The wet-inked series (Figure 2A, red traces) show consistently higher methylene asymmetric stretch intensities, which correlate to lower conformational uniformity, than SAMs in the saturation-inked series (Figure 2A, black traces). The mean and standard deviation for each series are shown by the data points and error bars to the right of the spectra. Peaks from SAMs produced by saturation-inked stamps have a narrower standard deviation than the wet-inked films. In the case of saturation inking, the stamp is returned to the inking solution between printing experiments.

We note an additional trend in the methylene stretch intensity for the wet-inked series. Reinking the stamp between each printing procedure increases ink loading and, thus, maintains ink concentration at the stamp/sample interface

with each subsequent print. This trend is apparent by tracking the observed 2919 cm^{-1} peak height versus the deposition sequence, as shown in Figure 2C, where each printed film shows higher conformational order than the preceding film.

In summary, saturation-inking improves the order and reproducibility of printed films over many samples and can be used to control their overall quality. This trend holds for all films printed with saturation-inked stamps; continuous control over absolute film quality can be obtained by the simple control of stamp interface concentration.

Control of Microdisplacement Printed Film Coverage. The **1AD** film is labile with respect to an *n*-alkanethiol ink with a chain length of at least eight carbon atoms. Alkanethiols are delivered by the stamp and insert into **1AD** SAM defect sites, gradually displacing the film *via* perimeter-dependent island growth.[42] Microdisplacement printing has three main advantages over direct printing on gold: limited indirect ink transport (via edge spreading or gas-phase deposition), viability of low-molecular-weight inks, and nanoscale chemical patterning produced by the emergence of fractal-like structures of two-component, partially displaced films. Our early efforts focused on producing fully displaced *n*-alkanethiolate films at the contact sites, as controlling fractional coverage as a function of printing time was imprecise because of variability of the ink concentration at the stamp/substrate interface. Figure 3 depicts SEM images of chemical patterns produced by the microdisplacement printing of 25 mM **C12** on a preformed **1AD** monolayer at several contact time intervals. Without an internal standard, the contrast mechanism for the SEM is not quantitative and provides little information regarding the nanoscale composition of the patterned films.[47,55] In previous work, we have used scanning probe microscopy imaging of chemical patterns, which were observed to be consistent with the more efficiently recorded SEM data shown here.

The initial displacement exchange rate is proportional to the square root of the *n*-alkanethiol concentration.[42] We use saturation-inking to maximize control over the displacement reaction and to monitor the kinetics of the process as well as relative coverage of mixed **1AD**/**C12** monolayer via IRRAS. The **1AD** IR spectrum has two main peaks, the CH_2 symmetric and asymmetric stretches at 2850 and 2911 cm^{-1}, respectively.[42,56] We have previously tracked the relative fractional coverage of two-component **1AD**/**C12** SAMs by monitoring the orientation-insensitive CH_3 symmetric stretch of **C12**[42,45,46] (and have also successfully utilized the same strategy for other cage-molecule assemblies[57,58]). Figure 4 shows the spectral evolution of a **1AD** SAM (Figure 4A) gradually displaced by **C12** delivered by a nonpatterned PDMS stamp (Figure 4B–E). The intensity of the adamantyl 2911 cm^{-1} stretch decreases concurrently with the emergence of the methyl symmetric and methylene asymmetric stretches, at 2877 and 2919 cm^{-1}, respectively. We use the methyl stretch to determine fractional coverage of mixed **1AD**/**C12** monolayers prepared with different stamp concentrations, the results of which are shown in Figure 5. The 25 mM ink concentration provided a good compromise of control and time at ~0.5% coverage per minute until >90% coverage. The higher and lower concentrations (50 and 10 mM, respectively) were inconvenient; displacement was too fast for fine control at high ink concentration, and lower concentrations did not provide sufficiently improved control over fine structure to justify the longer contact time.

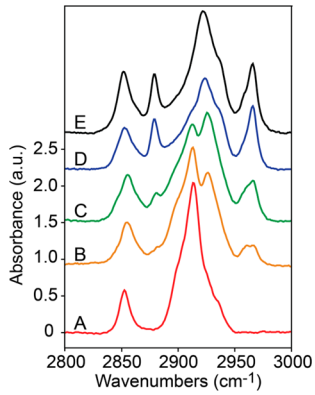

Figure 4. (A–E) Spectral evolution of 1-adamantanethiol (1AD) self-assembled monolayer (SAM) displacement. The preformed 1AD SAM is displaced gradually when held in contact with a PDMS stamp saturation-inked with 25 mM 1-dodecanethiol (C12). (A) Infrared spectrum of preformed 1AD SAM on Au. (B–E) Infrared spectra obtained after printing for 10, 100, 1000, and 10 000 s, respectively. (E) After 10 000 s of contact, the monolayer is a single-component C12 SAM.

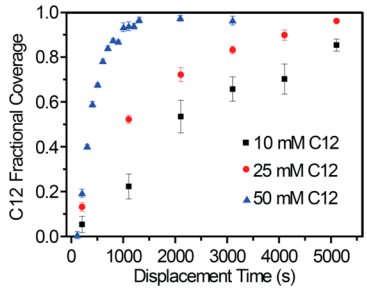

Figure 5. Fractional *n*-alkanethiolate self-assembled monolayer coverage by displacement printing at various ink concentrations. The 2877 cm^{-1} methyl symmetric stretch is analyzed to determine fractional 1-dodecanethiol coverage after partial displacement. At ~0.5% displacement per minute, the stamps that were saturation-inked with 25 mM 1-dodecanethiol proved the most convenient and reliable for fine control of fractional monolayer coverage by microdisplacement printing.

Modeling Diffusion of Molecular Ink at a Stamp Interface. In conventional μCP experiments, the stamp is placed in contact with a substrate for only a short printing time, usually about 30 s. Diffusion of ink into the stamp can be ignored as an important factor in these cases as the time required to obtain full monolayer coverage is short compared to the time scale for significant ink diffusion, and since increasing contact time tends to reduce pattern fidelity.[59–61] For experiments requiring longer contact times, however, ink diffusion into the stamp bulk becomes the determinant variable affecting performance and reliability of the technique.

A misconception regarding μCP ink transfer is that the polymeric stamp is coated only externally by ink. Although this is almost certainly the case for the transfer of nanomaterials, biomaterials, and polar molecular inks,[2,6,7,25,30,62,63] nonpolar *n*-alkanethiol inks dissolve readily in the PDMS, rather than pooling at the stamp surface.[64] The PDMS stamp medium can be thought of as a solvent of high viscosity.[65] Balmer et al. developed a model for the diffusion of *n*-alkanethiols in PDMS, and determined a diffusion coefficient of 5.0×10^{-7} cm^2 s^{-1} for 1-hexadecanethiol.[65] To illustrate the importance of effective flux at the stamp/substrate interface, we use their values, and a

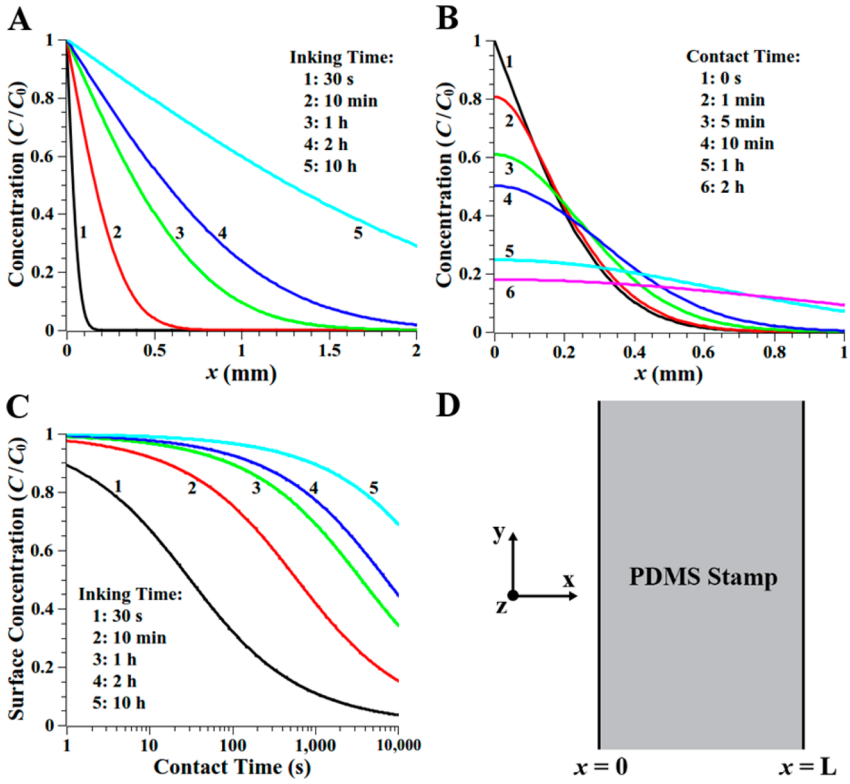

Figure 6. Model of linear one-dimensional diffusion of *n*-alkanethiol into a semi-infinite PDMS stamp. Plots depict concentration profiles of ink molecules within stamp as a function of position (depth beneath stamp surface) and time. (A) The ink reservoir maintains the stamp interface at a concentration of C_0 for all time $0 \le t \le T_{ink}$. The average diffusion length increases with the square root of inking time. (B) Concentration profile evolution (10 min inking time) after placing stamp in contact with an impermeable substrate. The interface concentration is no longer maintained at C_0, and the molecular ink diffuses further into the stamp. (C) Plot of ink concentration at the stamp/substrate interface as a function of contact time. Depletion by self-assembled monolayer deposition is neglected. Lower interface ink concentration corresponds to a lower effective flux, which in turn slows concentration dependent processes. Saturation-inking generates a concentration profile that varies less with position near the surface, and shows smaller changes in surface concentration in time, than wet-inking provides. (D) Schematic of the PDMS stamp used in the numerical model.

similar mathematical model, to approximate diffusion of *n*-alkanethiols of moderate length (**C12** and **C18**) in PDMS stamps.

We consider the diffusion of ink molecules into and within a PDMS stamp by numerically solving Fick's second law

$$\frac{\partial C}{\partial t} = D\frac{\partial^2 C}{\partial x^2} \tag{1}$$

using an iterative finite difference method. In eq 1, and in what follows, C represents the ink concentration, t is time, x is depth, D is the diffusion coefficient, and L is the thickness of the stamp. The stamp (as illustrated schematically in Figure 6D) is modeled as a semi-infinite medium that fills the space,

$$\text{stamp region} \begin{cases} 0 \le x < L \\ -\infty < y < +\infty \\ -\infty < z < +\infty \end{cases}$$

Henceforth, we will neglect the y and z dimensions because of the effectively infinite nature and symmetry of the stamp and only consider the diffusion in one dimension (x).

During inking, the exterior of the stamp ($x < 0$) is assumed to be an inexhaustible ink reservoir, of known concentration (C_0), that diffuses into the stamp. After a set amount of time, T_{ink}, the concentration of molecules within the stamp, as a function of position, is approximately

$$C(x, T_{ink}) = C_0 \text{erfc}\left(\frac{x}{2\sqrt{DT_{ink}}}\right)$$

in the limit where $L \gg 2(DT_{ink})^{1/2}$, where erfc() represents the complementary error function.[66]

After inking, the reservoir is removed and the faces of the stamp ($x = 0$, $x = L$) become impenetrable barriers through which no molecules may enter or leave. In the time that follows, the ink continues to diffuse throughout the stamp, causing the concentration profile to change in time. Figure 6A depicts five concentration profiles of alkanethiols in PDMS after inking for the specified time. The time evolution of the concentration profile for a stamp inked for 10 min is illustrated in Figure 6B.

A full-coverage *n*-alkanethiolate SAM on Au{111} is composed of approximately 4.6×10^{14} molecules per cm^2. Assuming a homogeneous, 25 mM ink distribution in a stamp, a full coverage monolayer may be formed from the molecules found within the first 0.31 μm beneath the stamp surface. For comparison, the *n*-alkanethiol diffusion length in PDMS is 14 μm after 1 s, and the short-term depletion by SAM deposition recovers in ~1 ms (vide infra). Therefore, ink depletion from deposition of a single SAM is negligible compared to that caused by diffusion over longer experimental time scales. However, if a stamp is to be used for multiple prints without reinking, ink depletion by SAM deposition becomes a more important variable with each print. Ink diffusion across the surface, away from the stamp-substrate contact region, occurs at

a much slower rate ($D_{Surface} \approx 1 \times 10^{-11}$ cm^2 s^{-1})[67] than diffusion into the bulk of the stamp and is thus neglected in this model.

Dynamic, concentration-dependent processes (e.g., molecular exchange between deposited molecules and molecules in PDMS) rely only on the concentration at the stamp/substrate interface, so we focus our attention on the depletion of ink at this interface and its relationship to inking time. Interface concentrations as a function of contact time are shown in Figure 6C for stamps inked for a range of periods. The further the ink penetrates into the stamp, the slower the rate of change at the interface during stamping; longer inking times maintain the initial interface concentration over longer experimental time scales. We reiterate that there remains sufficient ink near the interface to deposit a full-coverage SAM after an hour of diffusion, even for stamps inked for only a few seconds. Ethanol is known to cause PDMS to swell, linearly, by about 4% when fully saturated.[68] This swelling may subtly affect the final printed pattern; however, ethanol's swelling factor is relatively low compared to many other, less polar, solvents.

To summarize, ink concentration at the stamp/substrate interface depletes primarily by diffusion into the stamp interior. This becomes more significant as experimental time scales increase. For experiments involving stamping times over 1 h, ink concentration is best controlled by using a stamp of uniform concentration, although wet-inking methods can provide consistent results, provided long inking times. As a general rule, we immerse the stamp in an ink solution within a sealed vial for at least an order of magnitude longer than the planned contact time.

CONCLUSIONS AND PROSPECTS

Controlling transport phenomena is increasingly important for soft lithography. We have shown that by controlling the flux of ink at a stamp/sample interface, μCP and μDP can be used to produce films with control over composition, order, and reproducibility. We used a numerical model of one-dimensional ink diffusion into PDMS to illustrate the effect of ink depletion by diffusion into the stamp bulk as an important variable for long-duration patterning experiments. By saturation-inking, we can limit this variability and can prepare highly uniform SAMs with marked reproducibility and controllable crystallinity. These results are not limited to saturation-inking methodology; any method of inking the stamp that can produce a near-uniform concentration profile over the experimental time scale can be used effectively. We have shown the precision with which μDP printing can be used for the control of monolayer composition, enabling finely tuned chemical and physical surface properties across the macro-, micro-, and nanolength scales.

AUTHOR INFORMATION

Corresponding Author

*E-mail: psw@cnsi.ucla.edu.

Notes

The authors declare no competing financial interest.

ACKNOWLEDGMENTS

We acknowledge the financial support provided by the National Science Foundation through Grant CHE-1013042 and the Kavli Foundation.

REFERENCES

(1) Tien, J.; Terfort, A.; Whitesides, G. M. *Langmuir* **1997**, *13*, 5349−5355.
(2) Bernard, A.; Renault, J. P.; Michel, B.; Bosshard, H. R.; Delamarche, E. *Adv. Mater.* **2000**, *12*, 1067−1070.
(3) Fujihira, M.; Furugori, M.; Akiba, U.; Tani, Y. *Ultramicroscopy* **2001**, *86*, 75−83.
(4) Rogers, J. A.; Bao, Z.; Baldwin, K.; Dodabalapur, A.; Crone, B.; Raju, V. R.; Kuck, V.; Katz, H.; Amundson, K.; Ewing, J.; Drzaic, P. *Proc. Natl. Acad. Sci. U.S.A.* **2001**, *98*, 4835−4840.
(5) Jenkins, A. T. A.; Bushby, R. J.; Evans, S. D.; Knoll, W.; Offenhausser, A.; Ogier, S. D. *Langmuir* **2002**, *18*, 3176−3180.
(6) Porter, L. A.; Choi, H. C.; Schmeltzer, J. M.; Ribbe, A. E.; Elliott, L. C. C.; Buriak, J. M. *Nano Lett.* **2002**, *2*, 1369−1372.
(7) Santhanam, V.; Andres, R. P. *Nano Lett.* **2003**, *4*, 41−44.
(8) Geissler, M.; Wolf, H.; Stutz, R.; Delamarche, E.; Grummt, U. W.; Michel, B.; Bietsch, A. *Langmuir* **2003**, *19*, 6301−6311.
(9) Leufgen, M.; Lebib, A.; Muck, T.; Bass, U.; Wagner, V.; Borzenko, T.; Schmidt, G.; Geurts, J.; Molenkamp, L. W. *Appl. Phys. Lett.* **2004**, *84*, 1582−1584.
(10) Lange, S. A.; Benes, V.; Kern, D. P.; Horber, J. K. H.; Bernard, A. *Anal. Chem.* **2004**, *76*, 1641−1647.
(11) Kraus, T.; Stutz, R.; Balmer, T. E.; Schmid, H.; Malaquin, L.; Spencer, N. D.; Wolf, H. *Langmuir* **2005**, *21*, 7796−7804.
(12) Azzaroni, O.; Moya, S. E.; Brown, A. A.; Zheng, Z.; Donath, E.; Huck, W. T. S. *Adv. Funct. Mater.* **2006**, *16*, 1037−1042.
(13) Sharpe, R. B. A.; Titulaer, B. J. F.; Peeters, E.; Burdinski, D.; Huskens, J.; Zandvliet, H. J. W.; Reinhoudt, D. N.; Poelsema, B. *Nano Lett.* **2006**, *6*, 1235−1239.
(14) Burdinski, D.; Blees, M. H. *Chem. Mater.* **2007**, *19*, 3933−3944.
(15) Syms, R. R. A.; Zou, H.; Choonee, K.; Lawes, R. A. *J. Micromech. Microeng* **2009**, *19*, 025027.
(16) Wilbur, J. L.; Kumar, A.; Kim, E.; Whitesides, G. M. *Adv. Mater.* **1994**, *6*, 600−604.
(17) Biebuyck, H. A.; Whitesides, G. M. *Langmuir* **1994**, *10*, 4581−4587.
(18) Xia, Y. N.; Whitesides, G. M. *J. Am. Chem. Soc.* **1995**, *117*, 3274−3275.
(19) Xia, Y. N.; Mrksich, M.; Kim, E.; Whitesides, G. M. *J. Am. Chem. Soc.* **1995**, *117*, 9576−9577.
(20) Jeon, N. L.; Clem, P. G.; Nuzzo, R. G.; Payne, D. A. *J. Mater. Res.* **1995**, *10*, 2996−2999.
(21) Mrksich, M.; Whitesides, G. M. *Trends Biotechnol.* **1995**, *13*, 228−235.
(22) Jackman, R. J.; Wilbur, J. L.; Whitesides, G. M. *Science* **1995**, *269*, 664−666.
(23) Mrksich, M.; Chen, C. S.; Xia, Y. N.; Dike, L. E.; Ingber, D. E.; Whitesides, G. M. *Proc. Natl. Acad. Sci. U.S.A.* **1996**, *93*, 10775−10778.
(24) Smith, R. K.; Lewis, P. A.; Weiss, P. S. *Prog. Surf. Sci.* **2004**, *75*, 1−68.
(25) Perl, A.; Reinhoudt, D. N.; Huskens, J. *Adv. Mater.* **2009**, *21*, 2257−2268.
(26) Libioulle, L.; Bietsch, A.; Schmid, H.; Michel, B.; Delamarche, E. *Langmuir* **1999**, *15*, 300−304.
(27) Lahiri, J.; Ostuni, E.; Whitesides, G. M. *Langmuir* **1999**, *15*, 2055−2060.
(28) Donzel, C.; Geissler, M.; Bernard, A.; Wolf, H.; Michel, B.; Hilborn, J.; Delamarche, E. *Adv. Mater.* **2001**, *13*, 1164−1167.
(29) Kaufmann, T.; Ravoo, B. J. *Polym. Chem.* **2010**, *1*, 371−387.
(30) Vaish, A.; Shuster, M. J.; Cheunkar, S.; Weiss, P. S.; Andrews, A. M. *Small* **2011**, *7*, 1471−1479.
(31) Li, X.-M.; Péter, M.; Huskens, J.; Reinhoudt, D. N. *Nano Lett.* **2003**, *3*, 1449−1453.
(32) Scheres, L.; ter Maat, J.; Giesbers, M.; Zuilhof, H. *Small* **2010**, *6*, 642−650.
(33) Wendeln, C.; Rinnen, S.; Schulz, C.; Arlinghaus, H. F.; Ravoo, B. J. *Langmuir* **2010**, *26*, 15966−15971.
(34) Shestopalov, A. A.; Morris, C. J.; Vogen, B. N.; Hoertz, A.; Clark, R. L.; Toone, E. J. *Langmuir* **2011**, *27*, 6478−6485.

(35) Morris, C. J.; Shestopalov, A. A.; Gold, B. H.; Clark, R. L.; Toone, E. J. *Langmuir* **2011**, *27*, 6486−6489.
(36) Larsen, N. B.; Biebuyck, H.; Delamarche, E.; Michel, B. *J. Am. Chem. Soc.* **1997**, *119*, 3017−3026.
(37) Helmuth, J. A.; Schmid, H.; Stutz, R.; Stemmer, A.; Wolf, H. *J. Am. Chem. Soc.* **2006**, *128*, 9296−9297.
(38) Dameron, A. A.; Hampton, J. R.; Smith, R. K.; Mullen, T. J.; Gillmor, S. D.; Weiss, P. S. *Nano Lett.* **2005**, *5*, 1834−1837.
(39) Mullen, T. J.; Srinivasan, C.; Hohman, J. N.; Gillmor, S. D.; Shuster, M. J.; Horn, M. W.; Andrews, A. M.; Weiss, P. S. *Appl. Phys. Lett.* **2007**, *90*, 063114.
(40) Saavedra, H. M.; Thompson, C. M.; Hohman, J. N.; Crespi, V. H.; Weiss, P. S. *J. Am. Chem. Soc.* **2009**, *131*, 2252−2259.
(41) Liao, W.-S.; Cheunkar, S.; Cao, H. H.; Bednar, H. R.; Weiss, P. S.; Andrews, A. M. *Science* **2012**, *337*, 1517−1521.
(42) Saavedra, H. M.; Barbu, C. M.; Dameron, A. A.; Mullen, T. J.; Crespi, V. H.; Weiss, P. S. *J. Am. Chem. Soc.* **2007**, *129*, 10741−10746.
(43) Dameron, A. A.; Charles, L. F.; Weiss, P. S. *J. Am. Chem. Soc.* **2005**, *127*, 8697−8704.
(44) Dameron, A. A.; Hampton, J. R.; Gillmor, S. D.; Hohman, J. N.; Weiss, P. S. *Enhanced J. Vac. Sci. Technol., B* **2005**, *23*, 2929−2932.
(45) Mullen, T. J.; Dameron, A. A.; Saavedra, H. M.; Williams, M. E.; Weiss, P. S. *J. Phys. Chem. C* **2007**, *111*, 6740−6746.
(46) Dameron, A. A.; Mullen, T. J.; Hengstebeck, R. W.; Saavedra, H. M.; Weiss, P. S. *J. Phys. Chem. C* **2007**, *111*, 6747−6752.
(47) Srinivasan, C.; Mullen, T. J.; Hohman, J. N.; Anderson, M. E.; Dameron, A. A.; Andrews, A. M.; Dickey, E. C.; Horn, M. W.; Weiss, P. S. *ACS Nano* **2007**, *1*, 191−201.
(48) Hohman, J. N.; Claridge, S. A.; Kim, M.; Weiss, P. S. *Mater. Sci. Eng., R* **2010**, *70*, 188−208.
(49) Ulman, A. *Chem. Rev.* **1996**, *96*, 1533−1554.
(50) Love, J. C.; Estroff, L. A.; Kriebel, J. K.; Nuzzo, R. G.; Whitesides, G. M. *Chem. Rev.* **2005**, *105*, 1103−1170.
(51) Bumm, L. A.; Arnold, J. J.; Charles, L. F.; Dunbar, T. D.; Allara, D. L.; Weiss, P. S. *J. Am. Chem. Soc.* **1999**, *121*, 8017−8021.
(52) Nuzzo, R. G.; Dubois, L. H.; Allara, D. L. *J. Am. Chem. Soc.* **1990**, *112*, 558−569.
(53) Born, M.; Wolf, E. *Principles of Optics*, 2nd ed.; Cambridge University Press: Cambridge, U.K., 1999.
(54) Pan, S.; Belu, A. M.; Ratner, B. D. *Mater. Sci. Eng., C* **1999**, *7*, 51−58.
(55) Mack, N. H.; Dong, R.; Nuzzo, R. G. *J. Am. Chem. Soc.* **2006**, *128*, 7871−7881.
(56) Jensen, J. O. *Spectrochim. Acta, Part A* **2004**, *60*, 1895−1905.
(57) Kim, M.; Hohman, J. N.; Morin, E. I.; Daniel, T. A.; Weiss, P. S. *J. Phys. Chem. A* **2009**, *113*, 3895−3903.
(58) Hohman, J. N.; Zhang, P. P.; Morin, E. I.; Han, P.; Kim, M.; Kurland, A. R.; McClanahan, P. D.; Balema, V. P.; Weiss, P. S. *ACS Nano* **2009**, *3*, 527−536.
(59) Eberhardt, A. S.; Nyquist, R. M.; Parikh, A. N.; Zawodzinski, T.; Swanson, B. I. *Langmuir* **1999**, *15*, 1595−1598.
(60) Gannon, G.; Larsson, J. A.; Greer, J. C.; Thompson, D. *Langmuir* **2008**, *25*, 242−247.
(61) Bergmair, I.; Mühlberger, M.; Lausecker, E.; Hingerl, K.; Schöftner, R. *Microelectron. Eng.* **2010**, *87*, 848−850.
(62) Delamarche, E. *Chimia* **2007**, *61*, 126−132.
(63) Casero, E.; Petit-Dominguez, M. D.; Parra-Alfambra, A. M.; Gismera, M. J.; Pariente, F.; Lorenzo, E.; Vazquez, L. *Phys. Chem. Chem. Phys.* **2010**, *12*, 2830−2837.
(64) Delamarche, E.; Schmid, H.; Bietsch, A.; Larsen, N. B.; Rothuizen, H.; Michel, B.; Biebuyck, H. *J. Phys. Chem. B* **1998**, *102*, 3324−3334.
(65) Balmer, T. E.; Schmid, H.; Stutz, R.; Delamarche, E.; Michel, B.; Spencer, N. D.; Wolf, H. *Langmuir* **2005**, *21*, 622−632.
(66) We assume the diffusion length during inking is much less than the stamp's thickness. The physical interpretation of this condition is that, in the time allotted, a negligible amount of ink has diffused far enough into the bulk of the stamp such that it interacts with the far boundary. As such, we solve eq 1 for a stamp of infinite thickness.
(67) Sheehan, P. E.; Whitman, L. *J. Phys. Rev. Lett.* **2002**, *88*, 156104.
(68) Lee, J. N.; Park, C.; Whitesides, G. M. *Anal. Chem.* **2003**, *75*, 6544−6554.